


# Laser Linewidth Compression in Cascading Brillouin Random Fiber Lasers

Yikun Jiang, Liang Zhang , Haozhe Shou, Haoran Xie, Jilin Zhang, Yichun Li, Ying Zhang, Fufei Pang ,  
and Tingyun Wang 

**Abstract**—Cascaded Brillouin random fiber lasers (BRFLs) with laser linewidth compression were theoretically and experimentally demonstrated. Thanks to photon-phonon coupled interplay as well as randomly distributed feedback along silica fibers, the coherent time of cascading BRFL radiation is significantly prolonged whilst the phase noise is further suppressed, albeit with a quantum-noise-induced linewidth narrowing limit. To validate it, the linewidth narrowing ratio in BRFLs, defined as the ratio of the Brillouin pump and its sequent order of Stokes linewidth, was carried out and exhibited a dependence on the Brillouin pump linewidth, which is in good agreement with theoretical predictions. Furthermore, the relative intensity noises of cascading BRFLs were also investigated and discussed.

**Index Terms**—Random fiber lasers, stimulated Brillouin scattering, Rayleigh scattering.

## I. INTRODUCTION

ULTRA-narrow linewidth lasers with excellent properties of high temporal coherence and low frequency/phase noise play crucial roles in coherent communications [1], optical fiber sensing [2], [3], LIDAR [4], and laser interferometer-based gravitational wave detection [5]. For instance, the linewidth and frequency/phase noise of the laser source in optical fiber sensing systems determines the detection distance as well as the sensitivity [6]. Moreover, highly coherent lasers with narrow linewidth are beneficial to high-capacity and wide-coverage coherent communication systems, while a laser source with a broad linewidth will deteriorate the bit error rate in the channel [7].

Diverse techniques have been used to achieve narrow-linewidth lasers, including self-injection locking [8], [9], [10], Pound-Drever-Hall frequency stabilization [11], slow-light technology [12], [13], optical phase-locked loop [14], and Rayleigh

scattering-based feedback mechanism [15]. In particular, laser linewidth compression with 2~3 orders of magnitudes has been intensively verified in Brillouin cavity lasers [16], [17]. Since stimulated phonons with nanoseconds of lifetime decay faster than photons in the cavity, the stimulated Brillouin scattering (SBS) gain exhibits ultra-narrow bandwidth, benefiting the Brillouin lasers with highly coherent emission [18], [19]. To date, fiber cavity-based Brillouin lasers have been demonstrated to be capable of ~10 Hz ultra-narrow linewidth via single-frequency laser oscillation in a few meter short cavity [20]. Although the utilization of the short fiber cavity is conducive to suppressing the longitudinal mode of Brillouin lasing resonance, the laser threshold is inevitably increased and a high-precision spectral match between Stokes wavelength and the free spectral range corresponding to the cavity length is usually required [21].

Compared to conventional cavity lasers, Brillouin random fiber lasers (BRFLs), utilizing randomly distributed Rayleigh scattering as the feedback mechanism, facilitate cavity-less lasing radiation with ultra-narrow laser linewidth [22], [23]. It has been demonstrated that the laser linewidth of the BRFL pumped by a classical cavity-based laser can be remarkably compressed [24]. To further compress laser linewidth and upgrade laser noise performance of BRFLs, a number of researches have been proposed. For instance, a one-end pumping BRFL based on tapered fibers, instead of conventional single mode fibers, was demonstrated [25], in which Rayleigh scattering along tapered fibers was significantly enhanced to provide strong distributed feedback for highly efficient random lasing resonance. Alternatively, distributed random feedback from fiber-optic structures with artificially introduced disorder, *e.g.*, random fiber gratings [26], [27] were also used to overwhelm the traditional weak Rayleigh backscattering, yielding the coherent time extension of the generated laser photons with ultra-narrow linewidth. It has been demonstrated that the BRFL eventually allows a low-cost linewidth compressor with respect to a cavity-based pump laser of kHz linewidth, allowing ~75 Hz ultra-narrow linewidth random lasing radiation with a high side-mode suppression ratio [28]. Up to now, all previous BRFLs were investigated based on a classical cavity-based pump laser, meanwhile, the impact of the pump on the linewidth compression in cascading BRFLs remains ambiguous.

In this Letter, cascading BRFLs with half-open ring cavity structures were proposed and demonstrated. The theoretical framework of the linewidth compression in cascading BRFLs

Manuscript received 26 June 2022; revised 1 August 2022; accepted 11 August 2022. Date of publication 16 August 2022; date of current version 26 August 2022. This work was supported in part by the National Natural Science Foundation of China under Grant 61905138, in part by the Science and Technology Commission of Shanghai Municipality under Grant 20ZR1420800, in part by the State Key Laboratory of Advanced Optical Communication Systems and Networks under Grant 2022GZKF004, in part by Shanghai Professional Technology Platform under Grant 19DZ2294000, and in part by 111 Project under Grant D20031. (Corresponding author: Liang Zhang.)

The authors are with the Key Laboratory of Specialty Fiber Optics and Optical Access Networks, Joint International Research Laboratory of Specialty Fiber Optics and Advanced Communication, Shanghai Institute for Advanced Communication and Date Science, Shanghai University, Shanghai 200444, China (e-mail: henanyikun@163.com; liangzhang@shu.edu.cn; 863656059@qq.com; 351649836@qq.com; 1285882712@qq.com; 415958003@qq.com; yzhang9@shu.edu.cn; ffpang@shu.edu.cn; tywang@shu.edu.cn).

Digital Object Identifier 10.1109/JPHOT.2022.3199005

was developed by equivalent treatment on the optical path of the random cavity. Experimental results show that the linewidth narrowing ratio of cascading BRFLs depends on the linewidth of the Brillouin pump. Furthermore, the phase noise suppression of these cascading BRFLs was assessed by employing an unbalanced Michelson interferometer composed of a  $3 \times 3$  optical coupler. The relative intensity noises (RINs) were also characterized, exhibiting a reduced RIN transfer from the 1<sup>st</sup> to 2<sup>nd</sup> Stokes random lasing emission.

## II. THEORY

Determined by nanosecond phonon lifetime, the SBS gain in optical fiber has an extremely narrow bandwidth of 10~20 MHz, which benefits the Brillouin fiber laser with ultra-narrow linewidth performance. Theoretically, the linewidth of the Stokes laser  $\Delta v_s$  in a traditional Brillouin ring cavity can be governed by [29]:

$$\Delta v_s = \frac{\Delta v_p}{\left(1 + \frac{\pi \Delta v_B}{-cnR_c/nL_c}\right)^{2'}} \quad (1)$$

where  $\Delta v_p$  is the pump linewidth.  $R_c$  denotes the amplitude feedback parameter.  $c/n$  represents the light velocity in the fiber ring cavity with the length  $L_c$ . According to Eq. (1), the linewidth of the generated Stokes laser can be several orders of magnitude narrower than that of the pump. Note that,  $\Delta v_B$  is the full-width at half-maximum (FWHM) of the natural Brillouin gain spectrum  $g_B(v)$ , which should be replaced by that of the effective Brillouin gain spectrum  $\Delta v_B^{eff}$  in the case of the pump linewidth  $\Delta v_p$  with a comparable or larger bandwidth to  $\Delta v_B$ . In this scenario, the broadband pump eventually determines the effective Brillouin gain bandwidth as well as the lifetime of the provoked phonons.  $\Delta v_B^{eff}$  can be determined by the effective Brillouin gain spectrum  $g_B^{eff}(v)$ , which is the convolution of  $g_B(v)$  and the pump power spectrum [30]:

$$g_B^{eff}(v) = g_B(v) \otimes \frac{P_{pump}(v)}{P_{pump}^{tot}}, \quad (2)$$

where  $P_{pump}(v)/P_{pump}^{tot}$  is the normalization of the pump power spectrum.

Considering a BRFL with Rayleigh scattered random feedback, its fixed cavity has been removed. Thus, the abovementioned length of the cavity  $L_c$  is not valid, which however would be revised by the equivalent random cavity length  $L_r$ . In terms of a BRFL with a half-open ring cavity, the Stokes laser photons could unidirectionally propagate through the gain fiber ( $L_g$ ) in the main cavity while passing back and forth the Rayleigh fibers ( $L_R$ ). Thus, the equivalent random cavity length could be expressed as  $L_r = L_g + 2L_R^{eff}$ , where  $L_R^{eff}$  represents the effective length of the Rayleigh fiber. Meanwhile, the amplitude feedback parameter  $R_c$  in Eq. (1) should be replaced by Rayleigh random feedback parameter  $R_r$  in the BRFL.

Taking into account the intrinsic Stokes laser linewidth, the Stokes laser linewidth would never go narrower beyond the quantum noise limit even if the pump laser with the linewidth tending to 0. To address this issue, a correction factor

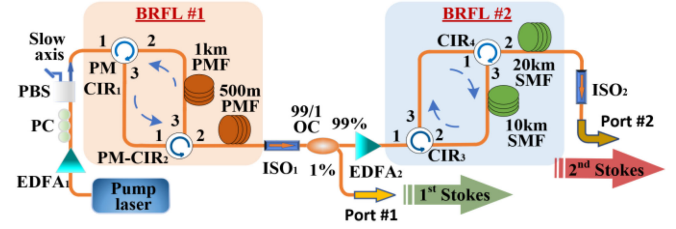


Fig. 1. Experimental setup of the cascading BRFLs.

$\alpha \Delta v_B^{eff}$  related to the effective Brillouin gain spectrum can be introduced for the derivation of the Stokes laser linewidth [28],

$$\Delta v_s^{BRFL} = \frac{\Delta v_p + \alpha \Delta v_B^{eff}}{\beta \left(1 - \frac{\pi \Delta v_B^{eff} n L_r}{c n R_r}\right)^2} \quad (3)$$

Here, the Rayleigh-induced compressed factor  $\beta$  is also introduced since distributed random feedback from numerous freezing Rayleigh scatters along long-span fibers can give rise to a Lorentzian envelope over the original frequency noise [32], benefiting salient phase noise suppression as well as an improved linewidth compression. According to Eq. (3), when the pump linewidth  $\Delta v_p$  approaches close to 0, the Stokes laser linewidth  $\Delta v_s^{BRFL}$  will tend to its limitation subject to the quantum noise in the BRFL.

## III. EXPERIMENTAL SETUP

Fig. 1 shows the schematic of the proposed cascading BRFLs, which consists of two independent half-open cavities (*i.e.*, BRFLs #1 and #2). A Laser beam from a pump (SE15, LAMDA) with the laser linewidth of 20 kHz is amplified by a commercial erbium-doped fiber amplifier (EDFA<sub>1</sub>) (EDFA-C-BA-23-B, YIXUN PHOTON) and then passes through a polarization controller (PC) and a polarization beam splitter (PBS) to deliver a linear polarization align to its slow axis. Then, the pump is injected into the BRFL#1 that consists of two polarization-maintaining optical circulators (PM-CIRs), two spools of 1 km and 500 m polarization maintaining fibers (PMFs) as Brillouin gain and Rayleigh fibers, which aims to emit the stabilized 1<sup>st</sup> Stokes laser against external disturbance. An isolator (ISO<sub>1</sub>) placed after the 500-m PMFs is used to remove any Fresnel reflection at the 1<sup>st</sup> Stokes laser output fiber surface. Afterward, 1% of the 1<sup>st</sup> Stokes laser is monitored by a 99/1 optical coupler (OC) at Port#1 while the 99% branch is subsequently launched into the BRFL#2 as its Brillouin pump which can be boosted by a second EDFA<sub>2</sub> (EDFA-C-BA-23-B, YIXUN PHOTON). In BRFL #2, another two spools of single mode fibers (SMFs) with longer lengths of 10 km and 20 km are utilized to provide higher Brillouin gain and Rayleigh feedback for more significant laser linewidth compression. Ultimately, the 2<sup>nd</sup> Stokes laser can be generated and detected at Port#2 when its pump reaches the laser threshold.

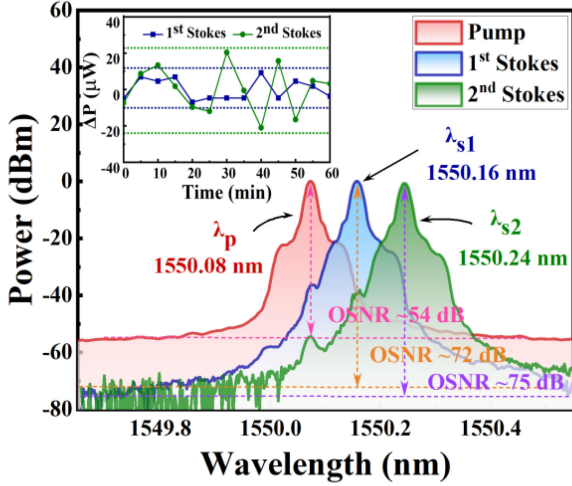


Fig. 2. Optical spectra of the pump, 1<sup>st</sup> Stokes and 2<sup>nd</sup> Stokes lasers. (Inset: power stability of 1<sup>st</sup> Stokes and 2<sup>nd</sup> Stokes within 1 hour.).

#### IV. RESULTS AND DISCUSSION

##### A. Laser Optical Spectrum

By adjusting two EDFAs, the injected pump power can be increased to overcome the laser thresholds of two stages of BRFLs and generate the 1<sup>st</sup> and 2<sup>nd</sup> Stokes laser, respectively. The lasing thresholds of the BRFL#1 and #2 are measured as 24.5 mW and 7.0 mW, showing a good agreement with theoretical calculations based on the SBS gain and Rayleigh scattering feedback [24].

The laser spectra and power fluctuations of cascading BRFLs are measured by an optical spectrum analyzer (AQ6370D, YOKOGAWA). In Fig. 2, the generated Stokes laser exhibits a Brillouin-induced wavelength upshift of 0.08 nm with respect to its pump. The optical signal-to-noise ratio (OSNR) of the 1<sup>st</sup> and 2<sup>nd</sup> Stokes exceeds over 70 dB which is around 20 dB higher than that of the pump laser. Furthermore, the power fluctuations of the Stokes lasers are recorded in 1 h with a time step of 5 min. As shown in the inset of Fig. 2, the power fluctuation of the 2<sup>nd</sup> Stokes in the SMF-based BRFL#2 is  $\pm 0.023$  mW within 1 hour while the power fluctuation of the 1<sup>st</sup> Stokes in PMF-based BRFL#1 is stabilized as  $\pm 0.012$  mW.

##### B. Laser Linewidth and Frequency Noise

To characterize the ultra-narrow laser linewidth of BRFLs (*i.e.*,  $< 1$  kHz), another identical random cavity was built to generate the same Stokes random laser emission with roughly identical phase noise as well as the linewidth. For the heterodyne linewidth measurement, the pump was split into two branches, between which a frequency shift of 80 MHz was introduced through an acousto-optic modulator. As a result, the heterodyne beat signals carrying the identical linewidth information of the Stokes random lasers occur at the center frequency of 80 MHz. In terms of the pump with a broad laser linewidth ( $> 10$  kHz), the delayed self-heterodyne (DSH) with delay fibers of 50 km was utilized for its measurement. The 3-dB linewidths are obtained through the Lorentz curve fitting of the heterodyne beat signals,

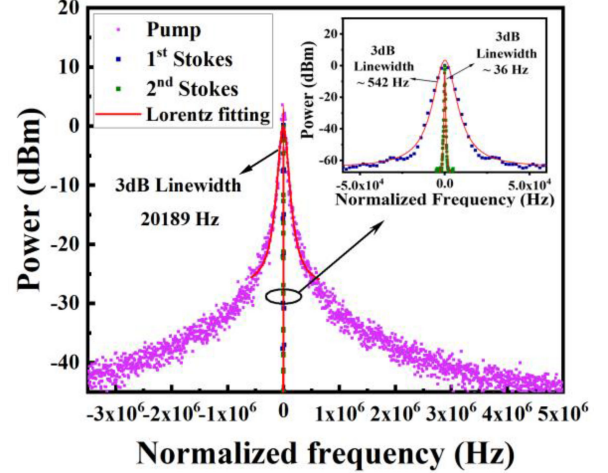


Fig. 3. Linewidth measurement with the heterodyne method. (The inset means the zooming in of the beat signals of the 1<sup>st</sup> and 2<sup>nd</sup> Stokes random lasers.).

as shown in Fig. 3. The 1<sup>st</sup> Stokes output from BRFL#1 exhibits the 3-dB linewidth of 542 Hz, while its pump shows the 3-dB linewidth of 20189 Hz. Furthermore, the 3-dB linewidth of the 2<sup>nd</sup> Stokes from the BRFL#2 is subsequently narrowed down to 36 Hz by one order of magnitude linewidth compression with respect to that of the 1<sup>st</sup> Stokes random laser.

Thanks to the acoustic lifetime far less than the characteristic time of Brillouin pump fluctuations in Brillouin gain medium [29], [31], the Stokes random laser linewidth compression of the BRFL is also confirmed with respect to the Brillouin pump. Moreover, the Rayleigh-induced phase noise suppression in BRFLs also benefits further linewidth narrowing to a large extent [32], particularly, for cascading BRFLs. It should be mentioned that the capacity of the linewidth compression is mitigated as the narrow-linewidth 1<sup>st</sup> Stokes random laser cascading to the 2<sup>nd</sup> BRFL, due to the intrinsic limit of the BRFL laser subject to the quantum noise, which originates from random phase noise of photons by spontaneous emission.

To characterize the phase noise of the cascading BRFLs, an unbalanced Michelson interferometer, composed of a  $3 \times 3$  optical fiber coupler and two Faraday rotator mirrors, was employed. The differential phase produced by the Michelson interferometer was demodulated and the frequency noise (FN) power spectral densities (PSDs) of different lasers were then calculated.

The FN PSDs of the pump, 1<sup>st</sup> Stokes and 2<sup>nd</sup> Stokes are shown in Fig. 4. It can be found that the FN of the 1<sup>st</sup> and 2<sup>nd</sup> Stokes random laser is much lower than that of the pump by over 20 dB, suggesting the phase noise suppression of the BRFL. Especially, the FN of the 2<sup>nd</sup> Stokes is further suppressed by cascading the 1<sup>st</sup> Stokes laser, which shows a good agreement with the above-mentioned linewidth measurements. Note that, the phase noise of the cascading BRFL towards the high-frequency domain ( $> 10^5$  Hz) tends to a limitation associated with the white noise  $S_0 \sim 10^{-2}$  Hz<sup>2</sup>/Hz. Hence, the intrinsic linewidth of the cascading BRFL can be estimated as  $\Delta\nu_s^{BRFL} = \pi S_0 \approx 0.03$  Hz.

According to the FN spectrum, the linewidth of lasers can be alternatively estimated based on the  $\beta$ -separation line approach



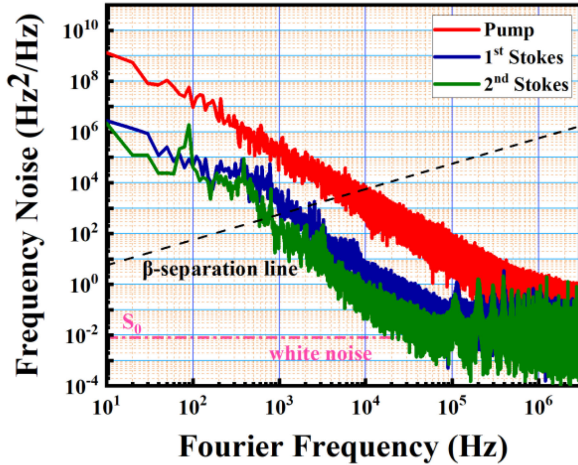


Fig. 4. The FN PSDs of the pump (red line), 1st Stokes (blue line) and 2nd Stokes (green line), respectively. The  $\beta$ -separation line (black dashed line) given by  $8\ln 2f/\pi^2$  while the white noise limit (magenta dot-dashed line) was also plotted.

TABLE I  
THE LASER LINEWIDTH MEASUREMENT

Laser source	Linewidth (Hz) (heterodyne)	Linewidth (Hz) ( $\beta$ -separation line)
Pump laser	20189	14670
1 <sup>st</sup> Stokes	542	601
2 <sup>nd</sup> Stokes	36	96

[33]. The FWHM of the laser linewidth can be derived by:

$$FWHM = \{8 \ln(2) A\}^{1/2} \quad (5)$$

Here,  $A$  is the integral area which can be expressed as:

$$A = \int_{1/T_0}^{\infty} H \left( S(f) - \frac{8 \ln(2) f}{\pi^2} \right) S(f) df. \quad (6)$$

$H(x)$  is the unit step function, and  $T_0$  represents the observation time that prevents the divergence of low frequency  $1/f^\alpha$  below  $1/T_0$ . Thus, the linewidths of different laser emissions can be deduced from the FN PSD curves in Fig. 4 by means of the  $\beta$ -separation line approach. Here,  $T_0$  of 2 ms is universally adopted in all laser linewidth measurements to eliminate low-frequency divergence induced by  $1/f^\alpha$  frequency noise [33]. The laser linewidth comparison of the pump, 1<sup>st</sup> and 2<sup>nd</sup> Stokes lasers obtained by the heterodyne and  $\beta$ -separation line approaches are listed in Table I, respectively.

To validate the dependence of the Stokes laser linewidth compression on the Brillouin pump, pump lasers with different linewidths, including commercial cavity-based lasers and the 1<sup>st</sup> Stokes random laser, were individually launched into the BRFL#2 to activate its next-order of Stokes random laser. Here, a linewidth narrowing ratio, defined as the ratio of the Brillouin pump to its subsequent order of Stokes linewidth, is introduced by  $\eta_{BRFL} = \Delta v_p / \Delta v_s$ . In Fig. 5, the linewidth narrowing ratio in BRFL#2 can be theoretically calculated according to Eq. (3) with the Rayleigh feedback parameter  $R_r$  of  $1.2 \times 10^{-4}$  and  $\Delta v_B$

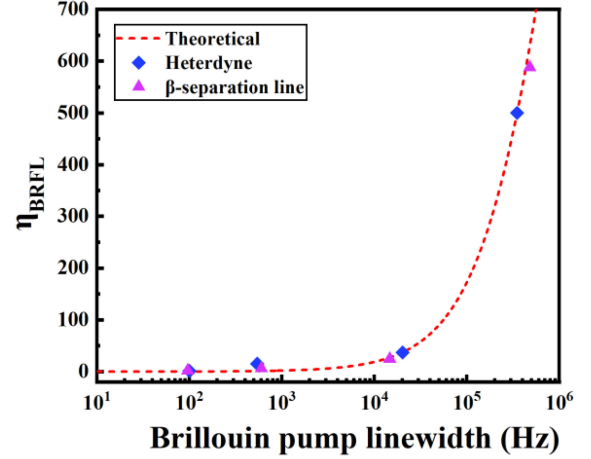


Fig. 5. The linewidth narrowing ratio  $\eta_{BRFL}$  versus the Brillouin pump linewidth in the BRFL.

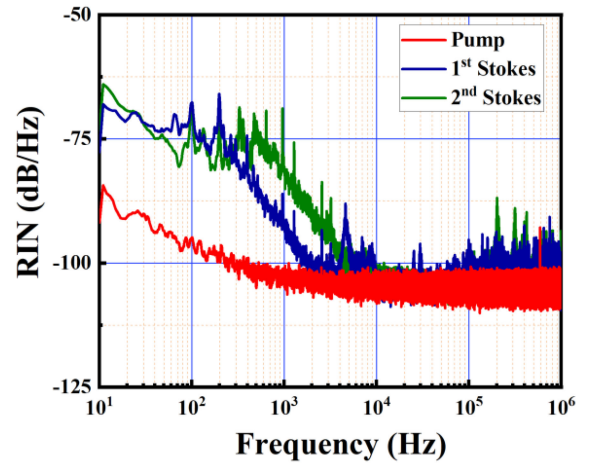


Fig. 6. The RINs of the pump, 1<sup>st</sup> and 2<sup>nd</sup> Stokes lasers.

of 20 MHz. The linewidth correction factor  $\alpha$  and Rayleigh-induced factor  $\beta$  are set as 0.0554 and 0.0067, respectively. The linewidth narrowing ratio  $\eta_{BRFL}$  reaches as large as around 500 when the laser linewidth of the Brillouin pump is  $\sim 300$  kHz, indicating superior linewidth compression with two orders of magnitudes. As the pump linewidth reduces towards as narrow as 100 Hz,  $\eta_{BRFL}$  tends to 1.2. Results confirm that the linewidth narrowing ratio  $\eta_{BRFL}$  in the BRFL gradually declines as a narrower linewidth laser is used as the Brillouin pump, showing a good agreement with the theoretical calculation. Note that, the output Stokes linewidth could be intrinsically convergent to the minimum (*i.e.*,  $\sim 0.03$  Hz) subject to quantum noise in the BRFL, particularly, in the case of cascading BRFLs.

### C. Relative Intensity Noise

The RIN characteristics of the pump and BRFLs were evaluated by recording the intensity fluctuations of Stokes light and analyzing the according PSD at the Fourier frequency range from  $10^1$  to  $10^6$  Hz. As shown in Fig. 6, the 1<sup>st</sup> and 2<sup>nd</sup> Stokes lasers show the average RIN increments of 5.7 dB and 5.2 dB

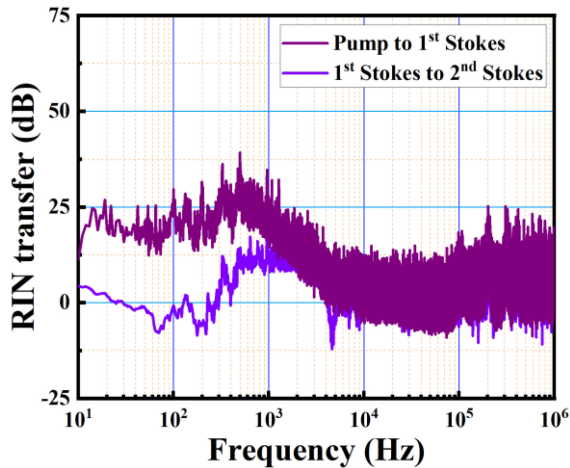


Fig. 7. The RIN transfer of BRFLs from the Brillouin pump to the subsequent order of Stokes.

than that of the commercial pump laser in the frequency range from 100 kHz to 1 MHz, respectively. However, the RINs of both 1<sup>st</sup> and 2<sup>nd</sup> Stokes lasers show a great rise (up to 25-dB higher) in the low-frequency region (10 Hz~5 kHz). Although this RIN increment is partially introduced by EDFAs, *i.e.*, < 2.5 dB within the frequency domain of less than 100 Hz, it predominantly attributes to the susceptibility of BRFLs to low-frequency external environmental disturbance including transient temperature variance and mechanical vibration. In particular, the BRFL#2, pumped by the BRFL#1, was conducted with SMFs and hence suffers from the inevitable polarization mismatch-induced Brillouin lasing resonance, resulting in ~10-dB higher RIN than that of BRFL#1 in the frequency range around 1 kHz.

In Fig. 7, the RIN transfer between a cavity-based pump laser and its corresponding 1<sup>st</sup> Stokes random laser exhibits a remarkable increment in the frequency range below 10<sup>3</sup> Hz, resulting from the natural superposition of the low-frequency intensity noise on the cavity-free BRFL. On the other hand, the 2<sup>nd</sup> Stokes laser shows a comparable low-frequency intensity noise to its 1<sup>st</sup> Stokes pump, leading to a reduced RIN transfer, in particular, in the low-frequency domain from 10 Hz to 300 Hz. It also suggests that the active physical isolation of ambient thermal noise and mechanical vibration would be effective for the suppression of the low-frequency RIN transfer in cascading BRFLs. It should be pointed out that, both RIN transfers (including pump-1<sup>st</sup> Stokes and 1<sup>st</sup> Stokes-2<sup>nd</sup> Stokes) exhibit similar trends in the high-frequency domain of above 10<sup>3</sup> Hz, indicating an intrinsic intensity fluctuation determined by numerous random mode competition in BRFLs, which could be further optimized by effective dilution of the random mode density, such as random fiber gratings [26].

To summarize, the cascading BRFLs exhibit robust frequency noise suppression and ultra-narrow linewidth compression, although the intensity noise of subsequent Stokes random laser is incremental in the manner of the RIN transfer. To address this issue, several approaches can be considered for further improvement. For example, short-length random fiber gratings with randomly distributed index modification can be utilized as

a compact enhanced random feedback to significantly reduce random mode density, benefiting a robust RIN suppression in random fiber lasers [34], [35]. Moreover, a self-inscribed transient population grating along unpumped Erbium doped fibers can be also capable of stabilizing the BRFL with improved intensity noise in the low-frequency domain [36].

## V. CONCLUSION

In this work, the linewidth compression of cascading BRFLs is theoretically and experimentally investigated. The theoretical framework of the laser linewidth of BRFLs is developed, predicting a cascading linewidth narrowing effect on the next-order Stokes random laser which is pumped by either a cavity-based or a cavity-free random laser. By performing the heterodyne and  $\beta$ -separation line methods, the laser linewidth and linewidth narrowing ratio  $\eta_{BRFL}$  of the cascading BRFLs were experimentally validated, corresponding well with predictions. Furthermore, the RIN transfer in BRFLs was also measured and discussed. It is believed that the proposed cascading BRFLs would arise interest in the laser fundamentals as well as the potential for practical applications such as long-haul coherent communications and ultra-sensitive fiber-optic sensing.

## REFERENCES

- [1] T. N. Huynh, F. Smyth, L. Nguyen, and L. P. Barry, "Effects of phase noise of monolithic tunable laser on coherent communication systems," *Opt. Exp.*, vol. 20, no. 26, pp. B244–B249, 2012.
- [2] X. Hu, W. Chen, X. Tu, Z. Meng, and M. Chen, "Theoretical and experimental study of suppressing stimulated Brillouin scattering and phase noise in interferometric fiber sensing systems with phase modulation," *Appl. Opt.*, vol. 54, no. 8, pp. 2018–2022, 2015.
- [3] Y. Li et al., "Thermal phase noise in giant interferometric fiber optic gyroscopes," *Opt. Exp.*, vol. 27, no. 10, pp. 14121–14132, 2019.
- [4] P. Benoit, S. Le Méhauté, J. Le Gouët, and G. Canat, "All-fiber laser source at 1645 nm for lidar measurement of methane concentration and wind velocity," *Opt. Lett.*, vol. 46, no. 1, pp. 126–129, 2021.
- [5] C. Cahillane, G. L. Mansell, and D. Sigg, "Laser frequency noise in next generation gravitational-wave detectors," *Opt. Exp.*, vol. 29, no. 25, pp. 42144–42161, 2021.
- [6] J. Qin et al., "Ultra-long range optical frequency domain reflectometry using a coherence-enhanced highly linear frequency-swept fiber laser source," *Opt. Exp.*, vol. 27, no. 14, pp. 19359–19368, 2019.
- [7] K. Kikuchi et al., "Characterization of semiconductor-laser phase noise and estimation of bit-error rate performance with low-speed offline digital coherent receivers," *Opt. Exp.*, vol. 20, no. 5, pp. 5291–5302, 2012.
- [8] L. Hao, X. Wang, K. Jia, G. Zhao, Z. Xie, and S. Zhu, "Narrow-linewidth single-polarization fiber laser using non-polarization optics," *Opt. Lett.*, vol. 46, no. 15, pp. 3769–3772, 2021.
- [9] N. T. Otterstrom et al., "Backscatter-immune injection-locked Brillouin laser in silicon," *Phys. Rev. Appl.*, vol. 14, no. 4, 2020, Art. no. 044042.
- [10] F. Wei et al., "Subkilohertz linewidth reduction of a DFB diode laser using self-injection locking with a fiber Bragg grating Fabry-Perot cavity," *Opt. Exp.*, vol. 24, no. 15, pp. 17406–17415, 2016.
- [11] P. Liu, W. Huang, W. Zhang, and F. Li, "Ultrahigh resolution optic fiber strain sensor with a frequency-locked random distributed feedback fiber laser," *Opt. Lett.*, vol. 43, no. 11, pp. 2499–2502, 2018.
- [12] Z. Pan, Q. Ye, H. Cai, R. Qu, and Z. Fang, "Fiber ring with long delay used as a cavity mirror for narrowing fiber laser," *IEEE Photon. Technol. Lett.*, vol. 26, no. 16, pp. 1621–1624, Aug. 2014.
- [13] Y. Shevy, D. Shevy, R. Lee, and D. Provenzano, "Slow light laser oscillator," in *Proc. Conf. Opt. Fiber Commun., Collocated Nat. Fiber Optic Engineers Conf.*, 2010, Paper OThQ6.
- [14] B. N. Jiang et al., "Low noise phase-locked laser system for atom interferometry," *Appl. Phys. B*, vol. 128, no. 4, pp. 1–5, 2022.

- [15] D. Xiang, P. Lu, Y. Xu, L. Chen, and X. Bao, "Random Brillouin fiber laser for tunable ultra-narrow linewidth microwave generation," *Opt. Lett.*, vol. 41, no. 20, pp. 4839–4842, 2016.
- [16] Z. Yuan, H. Wang, L. Wu, M. Gao, and K. Vahala, "Linewidth enhancement factor in a microcavity Brillouin laser," *Optica*, vol. 7, no. 9, pp. 1150–1153, 2020.
- [17] W. Loh et al., "Dual-microcavity narrow-linewidth Brillouin laser," *Optica*, vol. 2, no. 3, pp. 225–232, 2015.
- [18] H. H. Diamandi and A. Zadok, "Ultra-narrowband integrated Brillouin laser," *Nature Photon.*, vol. 13, no. 1, pp. 9–10, 2019.
- [19] N. T. Otterstrom, R. O. Behunin, E. A. Kittlaus, Z. Wang, and P. T. Rakich, "A silicon Brillouin laser," *Science*, vol. 360, no. 6393, pp. 1113–1116, 2018.
- [20] W. Loh, S. Yegnanarayanan, F. O'Donnell, and P. W. Juodawlkis, "Ultra-narrow linewidth Brillouin laser with nanokelvin temperature self-referencing," *Optica*, vol. 6, no. 2, pp. 152–159, 2019.
- [21] Y. Pang, Y. Xu, X. Zhao, Z. Qin, and Z. Liu, "Stabilized narrow-linewidth Brillouin random fiber laser with a double-coupler fiber ring resonator," *J. Lightw. Technol.*, vol. 40, no. 9, pp. 2988–2995, May 2022.
- [22] M. Pang, S. Xie, X. Bao, D.-P. Zhou, Y. Lu, and L. Chen, "Rayleigh scattering-assisted narrow linewidth Brillouin lasing in cascaded fiber," *Opt. Lett.*, vol. 37, no. 15, pp. 3129–3131, 2012.
- [23] M. Pang, X. Bao, and L. Chen, "Observation of narrow linewidth spikes in the coherent Brillouin random fiber laser," *Opt. Lett.*, vol. 38, no. 11, pp. 1866–1868, 2013.
- [24] M. Pang, X. Bao, L. Chen, Z. Qin, Y. Lu, and P. Lu, "Frequency stabilized coherent Brillouin random fiber laser: Theory and experiments," *Opt. Exp.*, vol. 21, no. 22, pp. 27155–27168, 2013.
- [25] S. Gao, L. Zhang, Y. Xu, P. Lu, L. Chen, and X. Bao, "Tapered fiber based Brillouin random fiber laser and its application for linewidth measurement," *Opt. Exp.*, vol. 24, no. 25, pp. 28353–28360, 2016.
- [26] Y. Xu, S. Gao, P. Lu, S. Mihailov, L. Chen, and X. Bao, "Low-noise Brillouin random fiber laser with a random grating-based resonator," *Opt. Lett.*, vol. 41, no. 14, pp. 3197–3200, 2016.
- [27] Y. Xu, P. Lu, and X. Bao, "Compact single-end pumped Brillouin random fiber laser with enhanced distributed feedback," *Opt. Lett.*, vol. 45, no. 15, pp. 4236–4239, 2020.
- [28] S. Huang et al., "Tens of hertz narrow-linewidth laser based on stimulated Brillouin and Rayleigh scattering," *Opt. Lett.*, vol. 42, no. 24, pp. 5286–5289, 2017.
- [29] A. Debut, S. Randoux, and J. Zemmouri, "Linewidth narrowing in Brillouin lasers: Theoretical analysis," *Phys. Rev. A*, vol. 62, no. 2, 2000, Art. no. 023803.
- [30] M. G. Herráez, K. Y. Song, and L. Thévenaz, "Arbitrary-bandwidth Brillouin slow light in optical fibers," *Opt. Exp.*, vol. 14, no. 4, pp. 1395–1400, 2006.
- [31] A. Debut, S. Randoux, and J. Zemmouri, "Experimental and theoretical study of linewidth narrowing in Brillouin fiber ring lasers," *J. Opt. Soc. Amer. B*, vol. 18, no. 4, pp. 556–567, 2001.
- [32] B. Saxena, Z. Ou, X. Bao, and L. Chen, "Low frequency-noise random fiber laser with bidirectional SBS and Rayleigh feedback," *IEEE Photon. Technol. Lett.*, vol. 27, no. 5, pp. 490–493, Mar. 2015.
- [33] G. Di Domenico, S. Schilt, and P. Thomann, "Simple approach to the relation between laser frequency noise and laser line shape," *Appl. Opt.*, vol. 49, no. 25, pp. 4801–4807, 2010.
- [34] Y. Li, P. Lu, X. Bao, and Z. Ou, "Random spaced index modulation for a narrow linewidth tunable fiber laser with low intensity noise," *Opt. Lett.*, vol. 39, no. 8, pp. 2294–2297, 2014.
- [35] Z. Zhou, P. Lu, L. Zhang, S. Mihailov, L. Chen, and X. Bao, "Thermal and acoustic noise insensitive Brillouin random fiber laser based on polarization-maintaining random fiber grating," *Opt. Lett.*, vol. 44, no. 17, pp. 4195–4198, 2019.
- [36] L. Zhang et al., "Frequency stabilized Brillouin random fiber laser enabled by self-inscribed transient population grating," *Opt. Lett.*, vol. 47, no. 1, pp. 150–153, 2022.